J. Phys. D: Appl. Phys. **32** (1999) 1–5. Printed in the UK PII: S0022-3727(99)07562-2

High power 4.6 μm light emitting diodes for CO detection

A Krier†, H H Gao†, V V Sherstnev‡ and Y Yakovlev‡

† Physics Department, Lancaster University, Lancaster LA1 4YB, UK
‡ Ioffe Physico-Technical Institute, St. Petersburg, 195279, Russia

Received 3 September 1999

Abstract. We report on a powerful 4.6 μm light emitting diode (LED), operating at room temperature, suitable for carbon monoxide gas detection. The source is based on a $InAs_{0.55}Sb_{0.15}P_{0.30}$ /$InAs_{0.89}Sb_{0.11}$/$InAs_{0.55}Sb_{0.15}P_{0.30}$ symmetrical double heterostructure with large band offsets. To improve performance, the $InAs_{0.89}Sb_{0.11}$ ternary material in the active region was purified by using rare-earth ion gettering during liquid phase epitaxial growth. A pulsed optical output power in excess of 1 mW at room temperature has been measured, making these emitters suitable for use in cost-effective instruments for the environmental monitoring of carbon monoxide.
The Auger coefficient of the $InAs_{0.89}Sb_{0.11}$ active region material was evaluated by analysis of the temperature quenching of the LED output power measured at constant current. It was found to be $C_0 = 1.5 \times 10^{-26}$ cm^6 s^{-1} with an activation energy of $E_\alpha = 31$ meV, which is in good agreement with previous findings in the literature.

(Some figures in this article appear in colour in the electronic version; see `www.iop.org`)

1. Introduction

The mid-infrared (2–5 μm) spectral range contains the strong fundamental molecular absorption bands of a number of combustible and atmospheric pollutant gases [1, 2]. Currently, infrared gas detection techniques based on optical absorption are becoming increasingly popular as they are the only ones which are truly gas specific and therefore reliable for gas sensor instrumentation [3–6]. Although some instruments which make use of thermal infrared sources already exist, the recent progress in developing room temperature light emitting diodes (LEDs) for the mid-infrared range holds considerable promise for extending the use of infrared methods still further [4] and for providing superior instrumentation. In order to obtain low detection thresholds and high signal-to-noise ratio (SNR) during the measurement of combustible and atmosphere pollutant gases, the output optical power of light sources used for such applications should be as high as possible. For CO detection at 4.6 μm in particular there is a need for a compact and efficient semiconductor light source which can provide emission beyond the cut-off wavelength of the glass envelope of a conventional filament bulb. Such an LED must operate at room temperature and have sufficient optical output ($\geqslant$ 1 mW) for it to be used in a practical gas sensor.

The ternary alloy $InAs_{1-x}Sb_x$ is a promising material for the production of mid-infrared light sources, because its room temperature energy gap covers the 3.5–5 μm spectral range when grown on near-lattice-matched InAs (or GaSb) substrates. Liquid phase epitaxy (LPE) of In-rich alloys onto GaSb is problematic due to substrate erosion by the In melt, whereas growth onto InAs substrates (for $\lambda_g = 4.6$ μm) has the disadvantage of lattice mismatch. Recently, we have reported on the epitaxial growth and fabrication of room temperature $InAs_{0.89}Sb_{0.11}$/$InAs_{0.55}Sb_{0.15}P_{0.30}$ semiconductor light emitting diodes operating at room temperature [7]. In that work, we made use of a strain compensating buffer layer of intermediate composition to accommodate the lattice mismatch. This approach proved to be successful and, as a result, an LED with an optical output power of 50 μW (using a 1 A pulsed current) was reported. However, we came to realize that the commercially available polycrystalline InAs and Sb metals, which are the basic precursor materials for LPE growth of such LEDs and detectors, contain residual donors of comparably high concentration. This can spoil the internal quantum efficiency of mid-infrared devices and is one factor which prevents the fabrication of mid-infrared LEDs with high optical output power at room temperature.

In this work, we report a further improvement in the electroluminescence quantum efficiency and LED performance. This was achieved by purification of the $InAs_{0.89}Sb_{0.11}$ epitaxial layer which forms the active region using a rare-earth ion gettering technique and by using purer source materials.

2. Experimental procedures

A horizontal multi-well sliding graphite boat in a Pd-diffused hydrogen atmosphere was used for the fully automated LPE growth of the material. The LED structures were grown onto 1 × 1 cm n-type InAs (100) substrates with 1×10^{18} cm^{-3} carrier concentration obtained from Wafer Technology Ltd. The LED structure, which has been described in detail previously [8], consists of two cladding layers of n^+

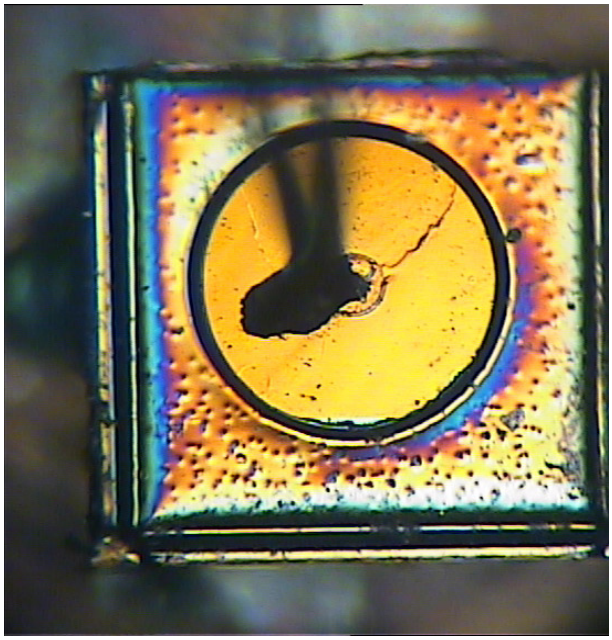

Figure 1. A photograph of a mesa-etched LED chip taken through a Nomarski microscope showing the mesa-etched structure (the dark region is the contact wire). The mesa diameter is 300 μm.

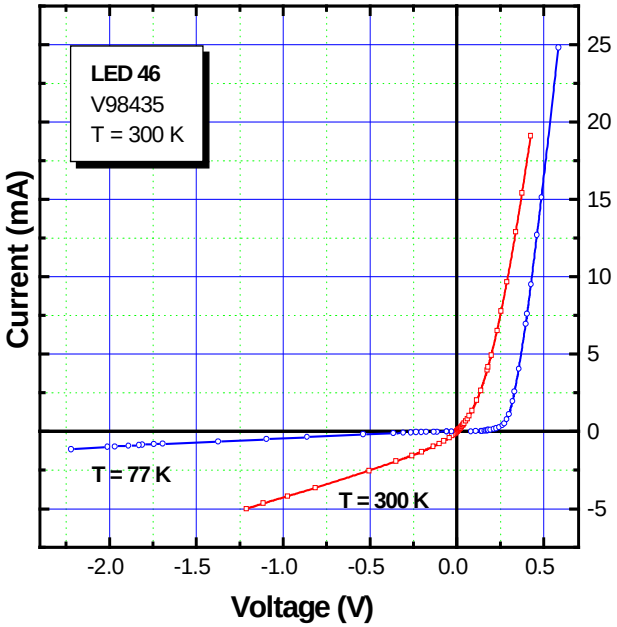

Figure 2. Current–voltage characteristics of one of the LEDs produced using monocrystal InSb and Yb gettering at 77 K and 300 K.

$InAs_{0.65}Sb_{0.15}P_{0.3}$ and p^+ $InAs_{0.65}Sb_{0.15}P_{0.3}$ and an undoped active region of $InAs_{0.89}Sb_{0.11}$ sandwiched between them. Because the $InAs_{0.89}Sb_{0.11}$ ternary active region material has a large lattice mismatch with respect to the InAs substrate layer, a buffer layer, with an intermediate composition ($InAs_{0.94}Sb_{0.06}$) having a 0.41% positive mismatch to the InAs substrate layer, was introduced in the structure between the substrate and the n-type $InAs_{0.65}Sb_{0.15}P_{0.30}$ layer in order to reduce dislocations and to relieve strain caused by the lattice mismatch.

The growth melts were prepared in a similar way to that of our previous report: 7N's pure indium, 6N's antimony and undoped polycrystalline InSb, InAs and InP were used to make up the melts. In this work, in order to investigate the effect of material purity on the quantum efficiency of the active region, four different types of devices were fabricated, in which the same epitaxial growth was used for each, but the nature of the antimony source material was different. The different precursors used in the growth melt of the active region were as follows: 6N's Sb metal, polycrystalline InSb, polycrystalline InSb + Yb and monocrystal InSb + Yb. The buffer layer was heavily doped (n-type) with Te up to 8×10^{18} cm^{-3} and was 4 μm in thickness. The quaternary cladding layers were doped to 4×10^{18} cm^{-3} n-type and 1×10^{18} cm^{-3} p-type using Te and Zn, respectively. The resulting epitaxial structures were processed using conventional photolithography and were mesa-etched into 300 μm diameter surface light emitting diodes. Ohmic contacts were formed by thermal evaporation of Au:Zn + Au on the p and Au:Te + Au on the n sides of the diode, respectively. Finally, the chips were mounted onto To49 headers for testing. A Nomarski microscope photograph of a typical mesa-etched LED chip is shown in figure 1.

3. Results and discussion

The I–V characteristics of a typical diode measured at 300 K and 77 K are shown in figure 2. The forward characteristics exhibit the usual exponential rise in current with applied voltage at both temperatures. Clearly the diodes are non-ideal and we obtained rather high values for the ideality factor in forward bias (e.g. 6.5 at 0.2 V). Such a high value of the ideality factor is believed to be due to series resistance effects [3]. We did not consider it a priority to minimize the series resistance of our LEDs in this work.

In order to investigate the effect of material purity on the quantum efficiency of the active region, we have investigated four different types of device. In each of these devices, the same epitaxial growth procedure was used to produce nominally the same structure. However, the nature of the antimony source material used was different, ranging from 6N's Sb metal, to monocrystal InSb + Yb, as mentioned above. In this experiment, we expect the improvement in precursor material purity (in going from metal to polycrystalline to monocrystal material) to result in increasingly pure epitaxial layers of InAsSb. The purpose of the Yb was to act as a gettering agent in the growth solution in order to remove S, Si impurities and to further improve the quantum efficiency of the layer.

Figure 3 shows the electroluminescence optical output power of these four types of device. The pulse current used for the comparison was 2 μs pulse duration at a frequency of 1 kHz. From these experimental curves, it can be seen that as the purity of the precursor used in the preparation of the active region goes up, the output power exhibits a large improvement. In fact, the output power of the device grown from monocrystal InSb and Yb was eight times larger than that grown from Sb metal at 2 A drive current. This phenomenon can be explained with reference to the well

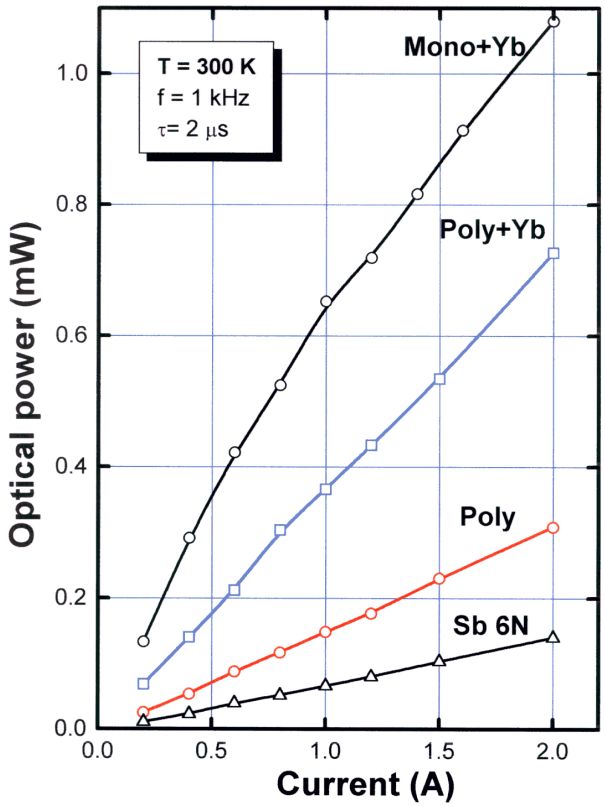

Figure 3. The optical output power characteristics measured from the different LEDs prepared with different purification treatments of the InAsSb active region.

known recombination equation which is typical for mid-infrared wavelength materials [9]:

$$P \propto R_{\mathrm{tot}} = q(A_{\mathrm{SRH}}\, n_{\mathrm{ac}} + B_{\mathrm{rad}}\, n_{\mathrm{ac}}^2 + C_{\mathrm{Auger}}\, n_{\mathrm{ac}}^3)\, h \qquad (1)$$

where n_{ac} is the carrier density in the active region, q is the electric charge, and h is the thickness of the active layer. The total recombination rate R_{tot} includes band-to-trap non-radiative recombination $A_{\mathrm{SRH}}n_{\mathrm{ac}}$ (Shockley–Read–Hall recombination), band-to-band radiative recombination $B_{\mathrm{rad}}n_{\mathrm{ac}}^2$ and Auger recombination $C_{\mathrm{Auger}}n_{\mathrm{ac}}^3$. The LED active region contains InAsSbP/InAsSb/InAsSbP interfaces and it is believed such interfaces can suppress Auger recombination, i.e. C in equation (1) [9–11]. But, in this work, we believe that, in addition to any possible reduction of Auger recombination, the reduction of the residual carrier concentration and defects, which reduce Shockley–Read–Hall recombination (A_{SRH}) in the active region, may be the most important contribution towards the large improvement in optical output power. We propose this primarily because we found similar improvements in our InAs LPE material grown using rare-earth (Gd) gettering technology [12, 13], where the photoluminescence intensity of Gd-treated InAs was improved by at least ten times compared to the undoped epitaxial InAs at low temperature.

Figure 4 indicates the optical output power dependence of the drive current pulse width of one typical device made from the monocrystal InSb + Yb precursor. It can be seen from the experimental result that the output power decreases

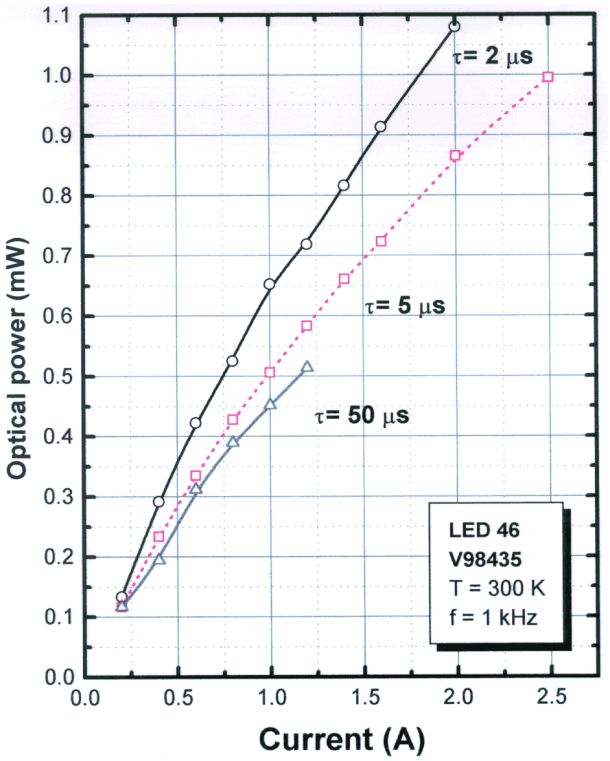

Figure 4. The optical output power characteristics measured using different current drive pulse widths for one of the LEDs produced using monocrystal InSb and Yb gettering.

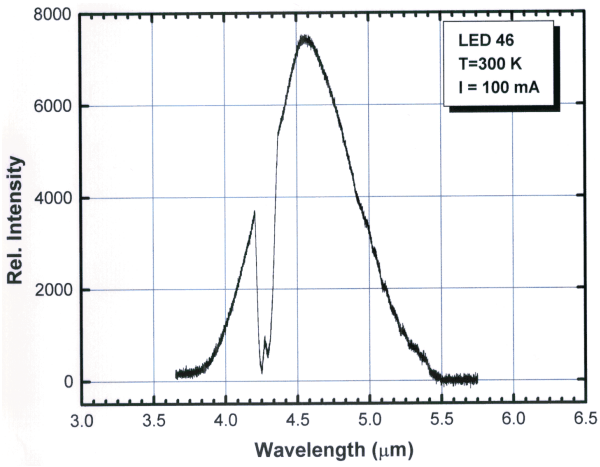

Figure 5. The room temperature electroluminescence emission spectrum obtained from one of the LEDs with a purified active region (InSb and Yb).

when the current pulse width increases. At constant 1.0 A pulse current, the output power goes down from 0.75 to 0.53 mW when the pulse width increases from 2 to 50 μs. This is because the drive current causes a rise in the active region temperature when the pulse width is larger than 2 μs. This is most likely to be associated with series resistance and Joule heating effects, but there may also be a contribution from carrier heating arising from Auger recombination.

Figure 5 shows the 300 K electroluminescence emission spectrum from one of the LEDs. The measurement was

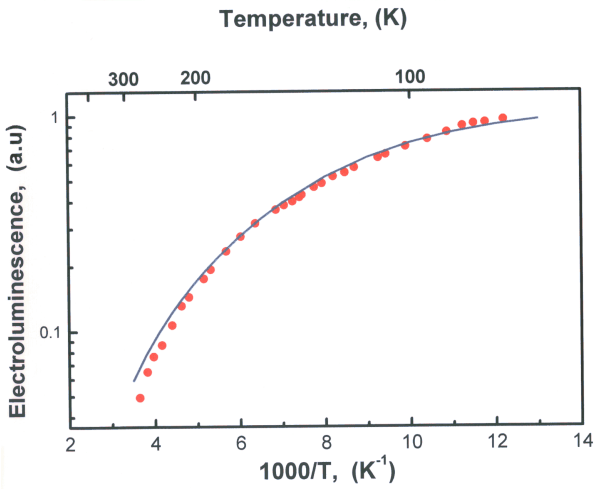

Figure 6. The optical output power dependence of inverse temperature for the LED of figure 5 normaliszd to 1 at 77 K. The solid curve represents curve fitting based on equation (1) to determine the Auger coefficient in the LED active region.

performed using a pulse current of 100 mA at 50% duty cycle. The absorption from atmospheric CO_2 at 4.2 μm is clearly visible and the LED emission has a peak wavelength of 4.6 μm. This is a little larger than we obtained in our previous work (i.e. 4.5 μm) [7]. We believe this is because the semiconductor material in the active region now contains fewer impurities and defects and is of higher crystalline perfection as a result of the purification. A slightly longer emission wavelength indicates a smaller energy bandgap, which is consistent with fewer shallow donor states and associated reduced Moss–Burstein band filling in the conduction band.

The temperature dependence of the LED optical output power intensity is shown in figure 6, where the electroluminescence intensity normalized to unity at 77 K, is plotted on a log scale versus inverse temperature ($1000/T$ K^{-1}). A constant 50 mA (50% duty cycle) excitation current was applied for this measurement throughout. From the experimental curve, it can be seen, that above 166 K, a rapid thermal quenching of the EL intensity was observed. Near room temperature, Auger recombination is believed to dominate in mid-infrared materials. Following other related research work [8], we estimated the Auger coefficient in the active region of our LED and its temperature dependence by fitting equation (1) to our experimental data. Since we have purified the active region, we are able to make the assumption that non-radiative band-to-trap recombination can be neglected, to a good approximation. The temperature dependence of B is known to be of the form $B(T) = B_0(T_r/T)$ according to the standard theory for radiative recombination [14]. In this work, T_r was set to 30 K, with $B_0 = 2 \times 10^{-10}$ cm^3 s^{-1}. The temperature dependence of C was assumed to be exponential and of the form $C(T) = C_0 \exp(-E_\alpha/kT)$ [15], where E_α is the activation energy for Auger recombination and C_0 is the Auger coefficient. The solid curve in figure 6 represents a fit to the experimental points measured from the temperature quenching of the electroluminescence emission intensity of the LED normalized to unity at 77 K. This assumes essentially that the Auger recombination becomes negligible at 77 K. The solid curve represents the best fit which was obtained using the above values of B_0 and T_r. We found that a reasonably good fit to our data was obtained when $C_0 = 1.5 \times 10^{-26}$ cm^6 s^{-1} and $E_\alpha = 31$ meV, implying that $C = 1.35 \times 10^{-28}$ cm^6 s^{-1} at 77 K and 4.5×10^{-27} cm^6 s^{-1} at 300 K respectively. The values of the Auger coefficient, $C_0 = 1.5 \times 10^{-26}$ cm^6 s^{-1} and the activation energy, $E_\alpha = 31$ meV are generally in good agreement with those obtained previously by other workers [8, 16, 17]. Figure 6 also shows that the purification method which we used was very effective in removing non-radiative recombination centres. The close proximity of the experimental points and the fitted curve indicates that the output power of these LEDs is effectively limited by the Auger process at all temperatures.

4. Conclusion

We have demonstrated that by using purified LPE material, it is possible to fabricate powerful LEDs which exhibit more than 1 mW of output power at room temperature in the mid-infrared at 4.6 μm. These LEDs are well matched to the CO absorption band and confirm the potential of these devices as being key components in infrared CO detection systems. A significant improvement (eight times) in output power of these LEDs has been achieved through purification of the active region by selecting different forms of Sb precursors and by using Yb gettering techniques. We attribute such effectiveness to the removal of traps and point defects from the active region. Also, the removal of unintentional donors from the material reduces the residual carrier concentration, which consequently reduces the bandgap slightly, resulting in LEDs which have their peak electroluminescence emission at 4.6 μm. The smaller carrier concentration produces less band filling and so the emission occurs presominantly from states closer to the band edges. Recombination from donor states is insignificant by comparison. Furthermore, through the measurement of LED output power dependence on temperature and simulation of the temperature quenching curve, the Auger recombination coefficient has been estimated as 1.35×10^{-28} cm^6 s^{-1} at 77 K and 4.5×10^{-27} cm^6 s^{-1} at 300 K, respectively. We have demonstrated clearly that the LEDs in this work are limited by Auger recombination.

Acknowledgments

We wish to thank EPSRC for the award of a visiting fellowship for V V Sherstnev. We also wish to thank Kidde International for supporting various aspects of this work.

References

[1] McCabe S and MacCraith B D 1993 Novel mid-infrared LED as a source for optical fibre gas sensing *Electron. Lett.* **29** 1719–21

[2] Gerritsen H 1974 Use of room temperature diodes in monitoring specific gases in air, particularly methane and carbon monoxide *Final Report* (US Department of Interior, Bureau of Mines) Contract No. 90101740, Grant No. G010740

[3] Parry M K and Krier A 1994 Efficient 3.3 μm light emitting diodes for detection methane gas at room temperature *Electron. Lett.* **30** 1968–69
[4] Popov A A, Sherstnev V V, Yakovlev Y P, Baranov A N and Alibert C 1997 Powerful mid-infrared light emitting diodes for pollution monitoring *Electron. Lett.* **33** 86–88
[5] Krier A and Mao Y 1997 2.5 μm light emitting diodes in $InAs_{0.36}Sb_{0.20}P_{0.44}$/InAs for HF detection *IEE Proc. Optoelectron.* **144** 355–59
[6] Popov A A, Stepanov M V, Sherstnev V V and Yakovlev Y P 1998 InAsSb light emitting diodes for the detection of CO_2 ($\lambda = 4.3\mu$m) *Tech. Phys. Lett.* **24** 596–98
[7] Gao H H, Krier A and Sherstnev V V 1999 InAsSb/InAsSbP light emitting diodes for detection of CO and CO_2 at room temperature *J. Phys. D: Appl. Phys* **32** 1768–72
[8] Kim S, Erdtmann M, Wu D, Kass E, Yi H, Diaz J and Razeghi M 1996 Photoluminescence study of InAsSb/InAsSbP heterostructures grown by low pressure metalorganic chemical vapor deposition *Appl. Phys. Lett.* **69** 1614–16
[9] Zegrya G G and Andreev A D 1995 Mechanism of Auger supperession in semiconductor hetrostructures *Appl. Phys. Lett.* **67** 2681–83
[10] Mikhailova M P, Moiseev K D, Berezovets Y A, Parfeniev R V, Bazhenov N L, Smirnov V A and Yakovlev Yu P 1998 Interface-induced phenomena in type II antimonide-arsinide hetrostructures *IEE Proc. Optoelectron.* **145** 268–74
[11] Zegrya G G, Mikhailova M P, Danilova T N, Imenkov A N, Moiscev K D, Sherstnev V V and Yakovlev Yu P 1999 Suppression of Auger recombinetion in diode lasers based on type II InAsSb/InAsSbP and InAs/GaInAsSb hetrostructures *Semiconductors* **33** 350–54
[12] Krier A, Gao H H and Sherstnev V V 1999 Purification of epitaxial InAs grown by liquid phase epitaxy using gadolinium gettering *J. Appl. Phys.* **85** 8419–22
[13] Gao H H, Krier A and Sherstnev V V 1999 High quality InAs grown by liquid phase epitaxy using Gd gettering *Semicond. Sci. Technol.* **14** 441–45
[14] Chinn S, Zory P, and Reisinger A 1988 *IEEE J. Quantum Electron.* **QE-24** 2191
[15] Gel'mont B, Sokolova Z, and Yassievich I 1982 *Sov. Phys. Semicond.* **16** 382
[16] Kane M *et al* 1996 Emission efficiency in InAs LEDs controlled by surface recombination *Boston MRS conference (December 1996)*
[17] Sugimura A 1980 Band-to-band Auger effect in GaSb and InAs lasers *J. Appl. Phys.* **51** 4405